The enrichment of CD44 in exosomes from breast cancer cells treated with doxorubicin promotes chemoresistance

xiaohong wang (wangxiaohong0607@126.com)
Binzhou Medical University hospital
kai cheng
Binzhou Medical University hospital
guoqiang zhang
Binzhou Medical University hospital
yue yu
Binzhou Medical University hospital
song liu
Binzhou Medical University hospital
yitong hua
Binzhou Medical University hospital
fengli guo
Binzhou Medical University hospital
xiaoqiang li
Binzhou Medical University hospital
weiwei zou
Binzhou Medical University hospital
hongguang sun
Binzhou Medical University hospital
shujian xu
Binzhou Medical University hospital
jianli dong
Binzhou Medical University hospital
zhenlin yang
Binzhou Medical University hospital

Research

Keywords: exosome proteomics, breast cancer, chemo-resistance, CD44

Posted Date: February 7th, 2020

DOI: https://doi.org/10.21203/rs.2.22928/v1

Version of Record: A version of this preprint was published at Frontiers in Oncology on July 14th, 2020.
See the published version at https://doi.org/10.3389/fonc.2020.00960.

Abstract

Background: Exosomes have been shown to be associated with chemotherapy resistance transmission between cancer cells. However, the cargo and function of exosomes changed in response to doxorubicin remains unclear.

Methods: We compared proteome profiles of exosomes extracted from the supernatant of MCF-7(S/Exo) and MCF-7/ADR(A/Exo) cells. We confirmed the differential expression of the candidate target-exosomic-CD44 by immune gold staining and western blot. We further studied the changes of chemosensitivity and CD44 expression in MCF-7 cells co-incubated with A/Exo. We analyzed the levels of exosomal CD44 from patient plasma, and compared the sensitivity and specificity of exosomic CD44 and plasma CD44 on diagnosis of chemoresistance. We modified the MCF-7-derived exosomes loaded with siRNA against CD44 to observe the effects of targeting reduced CD44 expression in lumimal A breast cancer cells.

Results: DOX increased the exosomes release from MCF-7/ADR cells and the exosomes mediated proteins intercellular transfer in breast cancer chemoresistance regulation. The candidate target of CD44 in A/Exo was much higher than in S/Exo and the increase levels of exosomic CD44 (21.65-fold) was much higher than cellular CD44 (6.55-fold). The same results were obtained in clinical samples. Exosome-siRNA targeted CD44 (Exos-siCD44) could efficiently targeted to silence its expression. When co-cultured on Exos-siCD44, breast cancer cells exhibited reduced cell proliferation and enhanced susceptibility to DOX and the same phenomenon was observed in mice.

Conclusion：Drug-resistant breast cancer cells spread resistance capacity to sensitive ones by releasing exosomes to transfer proteins in intercellular.

Background

Breast cancer is the most prevalent cancer among women and doxorubicin (DOX) is still the first-line clinical chemotherapy in breast cancer. However, doxorubicin therapy has a very low response rate (25–40%) owing to acquired drug resistance[1]. Thus, to analyze the crucial factors in the development of resistance of tumor cells is of great importance. Proteomics comparing analyses between drug-resistant and drug-sensitive MCF-7 cells identified that several proteins involved in apoptosis, the cell cycle, glucose metabolism, and fatty acid oxidation contribute to drug resistance[2–5] which could provides a good foundation for understanding the development of drug resistance in cell lines. Although the resistance-related proteins have been investigated and several metabolic pathways involved in MCF-7/ADR have been found[6], little is known about the global metabolic pattern and shift between the sensitive and resistant breast tumor cells.

Exosomes as membranous nanovesicles (30–150 nm size) of endocytic origin secreted by cells and carry along a wealth of cell-of-origin cargo and the cargo changes with cellular physiology and represents diagnostic opportunities for both tumor physiology mapping and cancer progression without accessing parent cells directly, which makes exosomes an attractive alternative as potential prognostic

biomarkers[7]. In recent years, exosome-induced chemoresistance is emerging as a novel mechanism[8]. Exosome signaling creates 'therapeutic tumor heterogeneity' and favorably condition tumor microenvironment[9, 10]. In the previous study, we also have found that the levels of exosomes released from doxorubicin-resistant breast cancer cells (MCF-7/ADR) are higher than MCF-7 cells and their transcriptome changes in response to doxorubicin[11]. Mechanistically, exosomes impart resistance by direct drug export, transport of drug efflux pumps and miRNAs exchange among cells[12]. However, the protein cargo and function of exosomes transmitted in response to doxorubicin remains unclear. Through the discovery of candidate biomarkers, mass spectrometry-based proteomics may provide a better understanding of the role of exosomes in intercellular chemoresistance transfer.

So in this study, we analyzed the proteome profile of the breast cancer line MCF-7 in dependence on doxorubicin resistance by LC-MS/MS. The finding of this study may serve to develop a potential therapy for chemotherapy resistance in breast cancer.

Materials And Methods

Cell culture

The human breast cancer cell lines MCF-7 was purchased from the Nanjing KeyGen. MCF-7 cells were induced by different concentrations of doxorubicin to establish resistance cell lines MCF-7/ADR. MCF-7 cells were cultured in RPMI-1640 medium supplemented with 10% exosome-depleted FBS. MCF-7/ADR were cultured in the medium containing 1ug/ml doxorubicin in order to maintain the drug resistant phenotype, and were then maintained in drug-free medium for at least two days prior to use. Cells tested negative for mycoplasma. All cells were maintained in 5% CO_2 at 37℃.

Exosomes isolation, identification and peptide extraction

To gauge the participation of exosomes in doxorubicin-induced transmission of drug-resistant, we used sequential ultracentrifugation to isolate exosomes from MCF-7 and MCF-7/ADR cells that were cultured in exosome-depleted medium for 48h. Exosome-depleted medium was prepared as follows: medium was ultracentrifuged for 16h, and then filtered using a 200-nm filter. Exosomes were identified by transmission electron microscopy (TEM) and ZetaView Nanoparticle-tracking analysis (NTA) instrumentation. To detect exosome-specific markers on isolated exosomes, purified exosome pellets were lysed with RIPA and quantified using NanoDrop (Thermo Scientific), and proteins were analyzed with an SDS-PAGE gel and detected using Odyssey® Infrared Imaging System(LI-COR). Samples were incubated with primary anti-CD63 (proteintech, 1:100) and anti-Calnexin antibodies (proteintech, 1:100), followed by IRDye® 800CW IgG (H+L) and IRDye® 680RD IgG (H+L) antibody (LI-COR, 1:15,000). The exosomes extracted from the supernatant of MCF-7 and MCF-7/ADR cells were named S/exo and ADR/exo, respectively. Protein separation, digestion and peptide extraction for LC-MS/MS were prepared according to the previous research methods[13]. The obtained peptides were labeled by TMT (Thermo Fisher Scientific, MA, USA) and cleaned, desalted and vacuum-dried.

Quantitative proteomic analysis and bioinformatic analysis

The obtained peptides from S/exo and A/exo were subsequently analyzed with an on-line two-dimensional nano LC/MS/MS by BioNovoGene. Scatter-plot matrices and density plots were created with the R programming language to verify the correlations between the data samples. The differently expressed proteins (DEPs) between S/exo and ADR/exo were selected by the difference multiples (log2|FoldChange|≧1.0) and significant levels (q-value<0.001). Then we performed GO enrichment analysis and KEGG pathway enrichment analysis as we described before[14].

Flow cytometry analysis of the differently expressed proteins

Given the low amount of exosomal protein, we chose flow cytometry analysis instead of western blotting to further verify the differently expressed proteins(log2|FoldChange|≧1.5). The collected exosomes were suspended by 100 μl PBS and attached to 10 μl aldehyde/sulfate latex beads (4 μm, A37304, Invitrogen, Carlsbad, CA, USA) for 2h continuous rotation at room temperature. This suspension was diluted to 1 ml PBS and rotated for 2h at RT. Centrifuge the suspension at 580 g for 5 min at RT and discard the supernatant. Resuspend the pellet with 1 mL of 100 mM glycine solution and incubate for 30 min at RT. Exosomes-bound beads were washed 1 time in 1× PBS/2% BSA and centrifuge for 1 min at 14,800 g, blocked with 10% BSA with rotation at room temperature for 30 min, washed a second time in 1× PBS/2% BSA and centrifuged for 1 min at 14,800 g and incubated with fluorescent antibodies (BioLegend□6 μl of antibody in 100 μl of 2% BSA/1× PBS) during 30 min rotating at 4°C. The percent positive beads were calculated relative to the CD63+ beads analyzed per sample and the log2|FoldChange| was calculated by the positive percentage.

Exosomal CD44 of breast cancer cells were detected by western blotting and immunogold labeling

To further validate the different level of CD44 in S/exo and ADR/exo, we performed immunogold labeling and western blot analysis which were conducted according to the previous protocol. Exosomes were fixed in 1% paraformaldehyde with 0.05 glutaraldehyde; The grids were immediately placed into the primary antibody of CD44 (Proteintech) at a 1:30 dilution and an isotype-matched negative control antibody for 36 h at 4℃. Then all of the grids were floated on drops of 6 nm gold particles (1:30 dilution) for 1 h at room temperature. Samples were then negatively stained with filtered aqueous 2% uranyl acetate for 1 min. Excess uranyl acetate was drained with filter paper and samples were examined on transmission electron microscope at an accelerating voltage of 120 Kv.

The effect on MCF-7 after incubation with ADR/Exo

To evaluate the changes of CD44 in MCF-7 after incubation with ADR/Exo, 1×10^6 MCF-7 cells were cultured in 6-well plates with different concentration (1×10^5, 1×10^6, 1×10^7, 1×10^8 and 1×10^9 particles/mL harvested at 7th day) and different time (1×10^8 particles/mL ADR/Exo harvested at 0,1st, 3rd, 5th and 7th day) continuous passage culture and added every other day. Cells were respectively harvested and stained with APC anti-human CD44 Antibody (BioLegend□CN. 338806□4 μL of antibody in 100 μL of 1×PBS) for 30 min at room temperature. APC-labeled IgG1κisotype controls (BioLegend□CN. 3400119) were used as negative controls. CD44 expression in MCF-7, MCF-7/ADR and MCF-7+ADR/Exo cell lines

was assayed by flow cytometry analysis. We further examined the DOX sensitivity of MCF-7 after 7 days incubation with 1×10^8 particles/mL ADR/Exo by CCK8.

Flow cytometry analysis of the levels of exosomal CD44 from patient plasma

To validate the exosomal CD44 as a diagnostic and predictive tool of response to DOX, peripheral blood samples were obtained from 54 patients with stage IIa-IIIc luminal A subtype breast cancer who were treated with neoadjuvant chemotherapy from January 2019 to December 2019 and the clinical data of the patients were collected. All the patients received neoadjuvant chemotherapy of epirubicin (75 mg/m^2, q21d) and docetaxel (75 mg/m^2, q21d) on day 1. All of the patients were followed-up until June 2019. The residual tumor burden was measured by magnetic resonance imaging (MRI) to evaluate the tumor response before surgical resection. The pathologic response was assessed according to the Response Evaluation Criteria in Solid Tumors (RECIST) criteria. Before the study, it was approved by the Chinese Clinical Trials Registry (Registration number is ChiCTR1900026195), and all patients were gave written informed consent (ethical vote number LW-012). The studies using human samples were designed as an explorative study. There was no interventional approach in this study. The plasma samples were collected from 28 patients responded to chemotherapy (PR/CR, partial response/complete response) and 26 patients did not respond (PD/SD, progressive disease/stable disease). All blood samples were taken before treatment and centrifuged at 2,500g for 10 min to extract the plasma, and the plasma was stored at -80°Cuntil analyzed. Exosomes isolated from human serum samples according to the protocols described before. 250 μL of cell-free serum samples were thawed on ice. Serum was diluted in 11 ml 1×PBS and filtered through a 0.2 μm pore filter. Afterwards, the samples were ultracentrifuged at 150,000g overnight at 4°C. Next, the exosomes pellet was washed in 11 ml 1×PBS followed by a second step of ultracentrifugation at 150,000g at 4°C for 2 h. The supernatant was discarded and pelleted exosomes were used for immunoelectron microscopy and flow cytometry analysis according to the previous research[15]. Via the method mentioned above, the exosomes-beads were incubated with CD63 Monoclonal Antibody (H5C6)-PE (Thermo Fisher Scientific, CN.12-0639-41) and APC anti-human CD44 Antibody (BioLegend□CN. 338806□6 μl of antibody in 100 μl of 2% BSA/1× PBS) during 30 min rotating at 4°C. Isotype Control incubation was used as control and to gate the beads with CD63+ and CD44+ bound exosomes respectively. The percent positive beads were calculated relative to the total number of beads analyzed per sample. This percentage was therein referred to as the percent beads with CD44+ exosomes. A paired two-tailed Student's t-test was applied to assay differences in percent bead with CD44+Exos in the longitudinal cohort between patients responded to chemotherapy and did not respond.

Enzyme-linked immuno sorbent assay (ELISA)

For further detection of CD44 on exosomes and patients' plasma, ELISA plates (96-well) (Biolegend) were coated with 0.25μg per well (100μl) of monoclonal antibody against CD44 overnight at 4°C. Free binding sites were blocked with 200μl of blocking buffer for 1 h at room temperature. Then, 100μl of plasma samples without exosome removal or exosome samples purified from plasma were added to each well.

The exosome supernatants were prepared by serial dilution according to the total protein level to analyse the enrichment of CD44 on exosomes. The concentration of CD44 was calculated based on the linear range of the ELISA assay data. Receiver operating characteristic curves (ROC) were used to determine the sensitivity, specificity, positive and negative predictive value and to compare area under the curves (AUC) of serum factors using the Delong method. The cut-off value was determined using the Youden-Index.

Construction of iRGD-Exosomes

To acquire modified exosomes that can target breast cancer cells, we established iRGD-exosomes. First, the iRGD peptide was cloned into Lamp2b, a protein expressed abundantly in exosomal membranes. Then, the plasmids encoding iRGD was transfected into MCF-7 cells using Lipofectamine 3000 transfection reagent according to the manufacturer's protocol (Invitrogen, USA). The medium was changed after transfection for 6 h, and the cells were incubated at 37 °C for 48 h to harvest the medium for density gradient centrifugation and NTA analysis as described above to obtained the iRGD-Exosomes. To validate whether iRGD-Lamp2b was transfected successfully into the MCF-7 cells, we assessed the levels of iRGD-Lamp2b mRNA 36 h after transfection using RT-PCR.

siRNA-CD44 encapsulation into exosomes by electroporation

Pre-chill the electroporation cuvette on ice for 30 min before electroporation. Mix 7.0 μg of exosomes (32 μL from 7 x 10^{12} p/mL stock in PBS) with 0.33 μg of siRNA (12 μL from 2 μM stock in RNase-free water) in the microcentrifuge tube. Make up the volume to 150 μL with citric acid buffer. The exosome to siRNA molar ratio is 1:60 in this case. Transfer the mixture to electroporation cuvette and rotate the turning wheel 180° clockwise.Then withdraw the sample from the cuvette with the plastic pipette and remove the free siRNA using size exclusion chromatography, and we obtained the iRGD-Exos-siRNA/CD44 (Exos-siCD44). The siRNA-CD44 sequence was GAAACT CCAGACC AGTTTA or Negative Control siRNA (siRNA-NC) sequence was TTCTCCGAACG TGTCACGT.

The exosome morphology changes were analyzed by TEM and NTA

The cell culture supernatant containing exosomes were harvested 48 h after transfection by centrifugation as described above. The exosome morphological integrity and size changes were analysed by TEM and NTA. The purified exosomes were re-suspended in PBS and stored at -80℃ prior to use. All procedures were carried out at 4℃.

Exosome labeling

We stained exosomes with the anti-CD63-Alexa Fluor 488 in vitro for cell uptake experiment and the lipophilic tracers 1,10 -dioctadecyl-3,3,30,30 -tetramethylindodicarbocyanine (DiD; Invitrogen, Carlsbad, CA) in vivo for animal imaging experiments. For CD63 labelling, the CD63-Alexa Fluor 488 antibody was added at a concentration of 1:50 and incubated for 30 minutes at 37°C. 4×10^8, 4×10^9 and 4×10^{10} exosomes were respectively incubated with DiD at the concentration of 10, 15, 20 and 25 μg/mL for 30

min at 37°Cto determine the optimal incubation conditions. Then ultracentrifuged at 120,000 g for 90 min to remove free dye. After being washed twice in PBS with 120,000 g centrifugation, the labeled exosomes were resuspended in PBS prior to use.

Role of iRGD-exosomes-siRNA CD44 on cell proliferation and drug resistance in MCF-7/ADR cells

The expression of CD44 on mRNA and protein levels in MCF-7/ADR cells after 24h and 72h incubation with Exos-siCD44 were detected by RT-PCR and western blot. The effects of silencing CD44 mediated by iRGD modified exosomes on DOX sensitivity of MCF-7/ADR cell were also measured by CCK-8 assay according to our previous test method. MCF-7/ADR cells were incubated with Exos-siCD44 and iRGD-exosomes-siRNA NC (Exos-NC) respectively for 12h, then cultured in 96-well plates with 2×10^4 cells per well overnight. After treatment with DOX for 48h, 20μL CCK-8 was added to each well and then incubated at 37 °C for 2 h. Absorbance values were then measured at 490nm using a microplate reader (Thermos). The sensitivity of the cells to DOX was measured by calculating the IC50 values. The experiment was repeated 3 times, each time with 3 parallel samples.

In vivo bioluminescence imaging and anti-cancer efficacy

6 week old female BALB/c nude mice were purchased from Beijing Vital River Laboratories and were housed in the SPF laboratory animal center of Binzhou Medical University Hospital. These mice were maintained under specific pathogen-free conditions at 22 ℃ under a 12-hour light-dark cycle and received standard chow and water ad libitum. All methods were approved by the Institutional Animal Care and Use Committee of Binzhou Medical University Hospital (No. SYXK 20180022). All experiments were conducted in accordance with the guidelines of the Ministry of Health of PR China and the Animal Care Committee of Binzhou Medical University. All efforts were made to reduce animal suffering and to minimize the number of animals used.

Human breast cancer cells (MCF-7/ADR, 1.0×10^7 cells in 50 μL PBS) mixed with 50 μL of matrigel were transplanted into the mammary fat pads of the mice, and allowed to grow to a tumor size ~0.1 cm^3 (volume=length×width^2/2, measured with a vernier caliper). The mice were then randomly divided into different experimental groups as described in Results. Did-labeled S/Exo were administered into tail veins of mice to study the biodistribution of exosomes. Biofluorescence images were obtained using an IVIS imaging system (PerkinElmer). Then, the ex vivo images were visualized from sacrificed mice using the IVIS imaging system.

iRGD-Exo-siRNA/CD44 were injected twice with an interval of 3 days, tumor sizes were measured every 3 days after the initial treatment, and tumors were excised from sacrificed mice at the end point of the experiments. To evaluate the expression of CD44, immunohistochemical staining was conducted using the excised tumors. 3 different fields under the microscope (×200) for each immunohistochemical slides were randomly chosen for scoring. Positive proportion and intensity were semi-quantitatively scored by 2 pathologists in a blinded manner.

Statistics

The GraphPad Prism version 8.0 was used for all calculations. A paired two-tailed Student's t-test was applied to assay differences in percent bead with $CD44^+$ Exos in the longitudinal cohort between patients responded to chemotherapy and did not respond. Receiver operating characteristic curves (ROC) were used to determine the sensitivity, specificity, positive and negative predictive value and to compare area under the curves (AUC) of serum factors using the Delong method. The cut-off value was determined using the Youden-Index. Figures were prepared by using GraphPad Prism 8. All presented *p* values are two-sided and $p<0.05$ was considered to be statistically significant.

Results

DOX induces exosomes release from MCF-7/ADR cells

We then examined the effects of chemotherapy on the release of exosomes from cancer cells. These vesicles expressed conventional exosomal markers CD63, while calnexin was only detected in total cellular lysates and not in exosomes (Fig. 1A), indicating that our exosomes preparations are free of cellular components and debris. NTA and TEM revealed a range of 121±5 nm and 117±4 nm in diameter, respectively ($p>0.05$) (Fig. 1B and C). Both exosomes revealed similar size distributions and morphologies. The concentration of exosomes was $(7.4\pm0.3)\times10^{11}$ Particles/g in A/Exo and $(4.2\pm1.5)\times10^{9}$ Particles/g in S/Exo ($p<0.05$) from the same volume of collecting cell supernatant (Fig. 1C). Our results show that treatment with DOX increased the exosomes release of MCF-7/ADR cells.

Proteomic analysis and bioinformatic analysis

The induced resistance capacity of chemotherapy-elicited exosomes may depend on their protein repertoire. We performed proteomic analysis of ADR/Exo and S/Exo using LC-MS/MS. In comparison with S/Exo, ADR/Exo showed a total of 250 different proteins, including 128 down-regulated proteins and 122 up-regulated proteins (Fig. 2A and Table 1-2). Then we further verified these differently expressed proteins by flow cytometry analysis which was consistent with the LC-MS/MS results (Fig. 2B). To investigate the functional basis of the identified chemotherapy-resistant proteins, GO analysis revealed that the differently expressed proteins mainly regulate cell-cell adhesion, cell-cell adherents junction, extra-cellular matrix organization, extra-cellular region and cadherin binding involved in cell-cell adhesion(Supplement date 1). KEGG analysis showed that the different proteins were mainly involved in the ECM-receptor interaction, Focal adhesion, complement and coagulation cascades, plate activation and PPAR signaling pathway (Supplement date 2).

DOX-elicited exosomes are enriched in CD44

It has been confirmed in our previous studies that CD44 played an important role in mediating chemoresistance and cell proliferation[16]. So in this study, we further studied the role of exosomic CD44 in the delivery of chemotherapy-resistance. Over-represented CD44 in ADR/Exo was confirmed under immune electron microscopy and the levels of CD44 in ADR/exo and S/exo were further detected by western blot. The results indicated that the protein level of CD44 was significantly up-regulated in

ADR/exo compared with that in S/exo (Fig 2C and D). Interestingly, the increase in the levels of CD44 by comparing ADR/exo and S/exo (14.76-fold) was much higher than that obtained by comparing MCF-7/ADR and MCF-7/S cells (6.56-fold) (Fig 2E), indicating that exosomes derived from MCF-7/ADR cells contained concentrated CD44, moreover, CD44 levels may be related to the DOX resistance transmission in breast cancer cells.

The expression of CD44 in MCF-7 after incubation with ADR/Exo

To evaluate the expression of CD44 in MCF-7 after incubation with ADR/Exo, we detected the CD44 expression in MCF-7+ADR/Exo at 0,1st, 3rd, 5th and 7th days by flow cytometry analysis. As is shown in Figure 3A-D, ADR/Exo incubation increased the expression of CD44 with dependence of concentration and time. The expression of CD44 in MCF-7+ADR/Exo with 1×10^5, 1×10^6, 1×10^7, 1×10^8 and 1×10^9 particles/mL was 5.73%±0.10%, 14.10%±0.70%, 63.00%±5.60%, 88.12%±9.70% and 92.0%±11.20% respectively. There was no significant difference between the 1×10^8 and 1×10^9 group (p>0.05), so we chose 1×10^8 particles/mL for the following study. The expression of CD44 in MCF-7+ADR/Exo at 0,1st, 3rd, 5th and 7th days was 4.35%±0.71%, 11.42%±1.60%, 33.21%±4.70%, 58.90%±6.54% and 91.10% ±9.66% respectively. The results showed that after treatment with ADR/Exo, there was a significant increase in the expression of CD44 (p<0.01). Especially after 7 days incubation, the expression of CD44 in MCF-7+ADR/Exo reached 91.10%±9.66%, while the expression of CD44 in MCF-7/ADR was only 77.30% ± 10.12%. The DOX sensitivity of MCF-7 was significantly decreased after 7 days incubation with 1×10^8 particles/mL ADR/Exo (Fig 3E) (p<0.05).

Higher levels of exosomal CD44 in PD/SD group

To explore whether CD44 can predict chemo-resistance in breast cancer patients, we assessed the levels of CD44 in the exosomes isolated from serum samples by immunoelectron microscopy and flow cytometry analysis. We used the RECIST criteria of pathological response to divide these patients into two groups: 28 patients responded to chemotherapy (PR/CR) and 26 patients did not respond (PD/SD). The results showed that exosomal CD44 in the serum of PD/SD was significantly higher than that in PR/CR (p< 0.0001, Fig. 3G-H). Immunogold TEM was used to confirm the specific CD44 expression and the results are consistent with the flow cytometry analysis results (Fig. 3F). Although limited, these data support the notion that the up-regulated CD44 in the circulating exosomes of patients played an important role in mediating chemotherapy resistance. ROC curves indicated that exosomal CD44 shows AUC=0.785, a sensitivity of 84.60% and a specificity of 78.60%, while serum CD44 shows an AUC of 0.576, a sensitivity of 53.80% and a specificity of 50.00% (Fig. 3I).

Isolation and characterization of iRGD-Exos

To validate whether iRGD-Lamp2b was transfected successfully into the MCF-7 cells, we assessed the levels of iRGD-Lamp2b mRNA 36 h after transfection using RT-PCR. Relative to untransfected MCF-7, the transfected MCF-7 cells expressed high levels of iRGD-Lamp2b mRNA. Then the purified exosomes were

electroplated and we obtained the Exos-siCD44. In the purified materials, typical exosome structures were observed by TEM and there were no significant changes in the morphological integrity after electroporation compared with the untreated exosomes (Fig. 4A). NTA also showed that the exosomes had a narrow size distribution, with a mean particle diameter of 117±7 nm for Exos-siCD44, and there were no significant difference in size compared with the untreated exosomes (Fig.4B). These characteristics indicate that the exosome properties were not affected by the modifications and electroporation. The levels of CD44 siRNA in exosomes were assayed by a LNA primer-based quantitative RT-PCR assay and the final concentration of CD44 siRNA was approximately 0.152 pmol/μg. The results clearly showed that CD44 siRNA can be effectively packaged into exosomes.

Targeting of iRGD-Exos in vitro and in vivo

To investigate whether iRGD-Exos are able to effectively bind to av integrin-positive cancer cells, iRGD-Exos or blank-Exos were labeled with Alexa Fluor 488-CD63 antibody and cultured with MCF-7 cells, which show high expression of av integrin-subunits on their surface. Confocal microscopy was used to observe the accumulation of CD63 (Alexa Fluor 488)-labeled exosomes in MCF-7 cells (Fig. 4C). It is likely that iRGD-Exo exhibited punctate signals, while blank-Exo showed fewer signals at 0.5h, 1h and 2h, respectively. The uptake efficiency was higher in the presence of iRGD-Exo than that in the presence of blank-Exo by mean fluorescence intensity analysis (MFI) (79.5%±11.2% versus 47.3%±8.6 at 2h, respectively).

Additionally, to determine whether two types of exosomes can target cancer tissue in vivo, DiD-labeled iRGD-Exo were intravenously injected into tail veins of MCF-7/ADR xenograft mice and observed 0, 2, 4, 6, 8, 12, 24 h post-inoculation using a bio-imaging system (Fig.4E). At the earliest time point studied (0.5h), the signal from iRGD-Exos was detected at the tumor sites, and peaked approximately 8 h after injection. Similar to in vitro uptake experiments, DiD-labeled iRGD-Exo significantly accumulated in tumor sites in vivo, while some were still detected in the liver and other tissues. Blank-Exo were detected less often in tumors compared with iRGD-Exo. Next, to confirm the accumulation of two types of exosomes in tumors, an ex vivo experiment was conducted at 8 h post-injection by sacrificing mice to dissect tumors and tissues (Fig. 4D). The vitro images showed that iRGD-Exo higher accumulated in tumors, although its accumulation was detected in liver tissue as well, while much less than blank-Exo. Thus, iRGD-Exo could be more efficiently uptaked by tumor cell.

siRNA silences CD44 expression in MCF-7/ADR cells

MCF-7/ADR cells were incubated with iRGD-Exos-siRNA/CD44 (Exos-siCD44) and Negative Control siRNA (Exos-NC). To validate the suppression of Exos-siCD44 on the CD44 of MCF-7/ADR cells, qRT-PCR and western blot were carried out. As shown in Fig. 4F, mRNA expression of CD44 in Exo-siCD44 group was significantly reduced compared with the Exos-NC group and untreated MCF-7/ADR group (p<0.05), and WB showed that the protein was reduced markedly in Exo-siCD44 group (p<0.05)(Fig. 4G). This indicates that Exos-siCD44 could effectively silence CD44 expression in MCF-7/ADR cells.

iRGD-exosomes-siRNA CD44 increased chemosensitivity in MCF-7/ADR cells

CCK-8 cell proliferation assay (Fig. 4H) revealed that optical density value (OD) of Exo-siCD44 treated MCF-7/ADR cells was significantly reduced in comparison with that of the Exos-NC group (0.420±0.020 vs 0.992 ± 0.103, $p<0.01$) ; the Exos-NC group and untreated MCF-7/ADR cells (0.892±0.125, $p>0.05$) have no significant difference. These results indicated that Exo-siCD44 increased DOX sensitivity in MCF-7/ADR cells and Exo-NC had no significant cytotoxicity.

In vivo anti-tumor efficacy of iRGD-Exos-siRNA/CD44

We next assessed the capacity of the Exo-siCD44 to inhibit tumor growth in tumor-bearing mice. Mice bearing established 0.1 cm^3 MCF-7/ADR tumors were randomly sorted into 6 groups (6 mice per group) and the groups were treated as follows: (i) PBS, as a control; (ii) Exo-NC; (iii) Exo-siCD44; (iv) Exo-siCD44 combined with weekly intraperitoneal DOX (4mg/kg) ; (v) equivalent dose of intraperitoneal DOX and (vi) equivalent dose of free siRNA/CD44. Treatments were given every other day for a total of 6 injections. Tumor volumes were measured every 3 days (Fig. 4I). From day 3 to day 21, the PBS-treated tumors increased 16.32-fold in volume, the DOX and free siRNA/CD44 alone treated tumors showed 9.51-fold and 11.42-fold increase in volume, whereas the Exo-siCD44 treated tumors showed only a 8.84-fold increase. DOX and Exo-siCD44 co-treatmented showed 4.12-fold increase, and there was no significant changes in Exo-NC group compared with PBS-treated group. No morbidity or mortality occurred following the 21-day treatment with Exo-siCD44, suggesting that Exo-siCD44 is not generally toxic to the animals under the experimental conditions used. Notably, the expression of CD44 was significantly decreased in Exo-siCD44 group compared with siRNA/CD44 group (Fig. 4J), further indicating the specific tumor targeting ability and anti-tumor activity of Exo-siCD44.

Discussion

DRUG RESISTANCE REMAINS ONE OF THE PRINCIPAL OBSTACLES IN THE TREATMENT OF CANCER AND FREQUENTLY CORRELATES WITH TUMOR RELAPSE, IN ADDITION TO POOR PATIENT OUTCOMES. Previous studies have shown that the diverse biological functions of exosomes as vectors of signaling molecules that can deliver their cargo to adjacent or distant cells and can alter pathways and processes affecting cell chemotherapeutic sensitivity[17, 18]. Mechanistically, exosomes impart resistance by direct drug export, transport of drug efflux pumps and miRNAs exchange among cells. Genomic and transcriptomic profiles of exosomes mediated chemoresistance have been well established[19–21], however the proteomic contribution to these profiles has yet to be elucidated. In this work, characterising the exosomal protein components from drug resistant cells will improve our understanding on their role in the progression of chemoresistance transmission.

In this study, we firstly examined the effects of DOX on the release and biological function changes of exosomes. Then proteomics was employed to profile the intracellular information transfered by exosomes between MCF-7/ADR and MCF-7 cells. Some potential biomarkers were identified and the

metabolic pathways were analyzed to illustrate the mechanisms of drug resistance transmission. Potential markers identified can be used for evaluating the pharmacodynamics and exploring the mechanisms of tumor cells resistant to DOX. OUR RESULTS INDICATE THAT CHEMOTHERAPY-RESISTANT TUMOR CELLS SELECTIVELY SHUTTLED THEIR SECRETED SPECIFIC PROTEINS INTO EXOSOMES AND THAT EXOSOMES TRANSPORT AND DELIVER THESE PROTEINS TO OTHER TUMOR CELLS. 250 DIFFERENTIALLY EXPRESSED PROTEINS WERE FOUND IN ADR/EXO COMPARED WITH S/EXO. THE HIGHER LEVEL OF CHEMOTHERAPY-RESISTANT PROTEINS THAT ABCB1, CD44, GSTP1, PAICS, AXL, ANXA2, HSPB1, ICAM1 AND MMP-1 ETC AND THE LOWER LEVELS OF LOX, HIC2, HRG, COL1A1, HTRA1, AEBP1 AND MAP2K5 PROTEINS RELATED WITH THE ENHANCED DRUG SENSITIVITY AND GROWTH SUPPRESSION OF CANCER CELLS WERE CONCENTRATED IN ADR/EXO. This work presented here shows the added value of exosomes proteomics, both independently as a robust methodology and as a complementary layer of biological information to genomics and transcriptomics.

IN THE PREVIOUS STUDY, WE HAVE FOUND THAT THE PERCENTAGE OF CD44 + CELLS IN THE MCF-7 CELL LINE IS EXTREMELY LOW. INTERESTINGLY, iN THIS STUDY, WE FOUND THAT DOXORUBICIN INDUCED THE SECRETION OF EXOSOMES AND INCREASED THE ENCAPSULATION OF CD44 IN EXOSOMES IN MCF-7 CELLS. CD44 as the receptor for hyaluronic acid (HA), a major component of the extracellular matrix (ECM), mediated intracellular cell signaling through its interaction with cytoskeletal proteins and involved in cell adhesion, migration, drug resistance, and signal transmission in some drug-resistant cancer cell lines[22–25]. Recent studies have demonstrated that the targeted down-regulation of CD44 can significantly enhance the cisplatin sensitivity of chemoresistant NSCLC cells[26]. So targeting CD44 using anti-CD44 and/or CD44 variant-specific antibody and/or anti-sense strategies to downregulate CD44 and/or CD44 variants may be a possible choice for the development of new cancer cell-based therapies. Our data showed that DOX-resistant cells could transfer resistance properties to DOX-sensitive counterparts and that this behavior is partly mediated by exosomal CD44. Interestingly, co-incubation with Exo-siCD44 significantly increased sensitivity to chemotherapy in MCF-7/ADR cells and tumor-bearing mice but barely affected after Exo-NC, suggesting that exosomal CD44 played an important role for the MCF-7 cells acquired DOX resistance. Therefore, it is important to elucidate the role of CD44 in the development of chemoresistant and develop effective therapeutic strategies to overcome chemoresistance.

As exosomes naturally carry RNA between cells, it could deliver therapeutic short interfering RNA (siRNA) to target cells. Normally, exogenous RNA is prone to degradation via RNAse, has a limited ability to cross cell membranes due to the negative charged surface and may induce an immune response. Exosomes can overcome these limitations. In our study, we used MCF-7 cells as a source of exosomes (S/exo), as cancer-derived exosomes have been reported to be used as a delivery platform which could confer cancer cell tropism-dependent targeting[27]. The tumor targeting capability of S/exo were further conferred by engineered to express lysosome associated membrane glycoprotein 2b (Lamp2b), a well-characterized exosomal membrane protein, fused with iRGD targeting peptide for av integrin. We established the delivery vehicle for the disruption of CD44 expression by tumor-derived exosomes loaded with siRNA against CD44. Our results demonstrated that iRGD-Exos had specific targeting in vitro and in vivo. And

loaded with siRNA/CD44, iRGD-Exos-siRNA/CD44 could inhibit the cell proliferation in vitro and inhibit tumor growth in tumor-bearing mice. Exosomes, as a natural nanocarrier, have great potential as a cancer therapy. However, more work is still needed, especially for in vivo studies and clinical trials. Exosomes derived from cancer cells carry functional cargos which directly or indirectly facilitate tumor cell growth. Therefore, how to identify and remove those tumor supporting components from exosomes is critical for exosome-mediated cancer therapy.

Conclusions

The resistance-related proteins have been investigated and several metabolic pathways involved in chemo-resistance have been found in breast cancer little is known about the global metabolic pattern and shift between the sensitive and resistant breast tumor cells. In this study, we confirmed that DOX-resistant breast cancer cells spread resistance capacity to sensitive ones by releasing exosomes to transfer resistance-associated proteins. Exosomes have the role of a double-edged sword, while transmitting drug resistance information, they can also efficiently target tumor cells to play the role of therapeutic vectors. The discovery of candidate biomarkers, mass spectrometry-based proteomics may provide a better understanding of the role of exosomes in intercellular chemo-resistance transfer and offer a great value in clinical diagnosis, monitoring and treatment for chemo-resistance of breast cancer.

Abbreviations

A/Exo, exosomes extracted from MCF-7/ADR cells

CR, complete response

DEPs, the differently expressed proteins

DOX, doxorubicin

GO analysis, gene ontology analysis

LC-MS/MS, liquid chromatography linked to tandem mass spectrometry

MCF-7/ADR, doxorubicin resistance MCF-7 cells lines reduced by adriamycin

MDR, multidrug resistance

NTA, ZetaView Nanoparticle-tracking analysis

PD, progressive disease

PR, partial response

SD, stable disease

S/Exo, exosomes extracted from MCF-7 cells

Declarations

Ethical approval and consent to participate

The study was conducted in accordance with the guidelines in the Declaration of Helsinki and it has been approved by the Chinese Clinical Trials Registry (Registration number is ChiCTR1900026195) and Medical Research Ethics Committee of Binzhou Medical University Hospital (Approval No. LW-012). All consents were obtained.

Consent for publication

The manuscript does not contain any identifiable individual person's data in any form. The provided dataset is fully anonymous. All authors consent to publication of the manuscript.

Availability of data and material

The datasets used and/or analyzed during the current study are available from the corresponding author on reasonable request.

Competing interests

The authors declare that no conflicts of interest exist with regard to this manuscript.

Funding

This work was supported by National Natural Science Foundation of China (NO.81902702, NO.81173601 and No.31801085), Natural Science Foundation of Shandong Province (NO.ZR2017LH072 and NO.ZR2017MH033), Projects of Binzhou technology development program (NO.2015ZC0301), National Key Research and Development Project (NO.2018YFC0114705), Scientific Research Staring Foundation of Binzhou Medical University (NO.BY2014KYQD36, NO.BY2014KJ36 and NO.BY2017KJ01), Science and Technology Program of Universities in Shandong Province (No. J15LL51).

Author Contributions

Xiaohong Wang designed the experiments, performed the experiment, analyzed results and wrote the manuscript. Kai Cheng, Guoqiang Zhang, Yue Yu, Song Liu, Yitong Hua and Xiaoqiang Li performed the experiments and analyzed the results. Weiwei Zou, Hongguang Sun and Shujian Xu summarized the clinical data and performed the statistical analysis. Fengli Guo and Jianli Dong revised the manuscript. Zhenlin Yang designed the experiments and revised the manuscript.

Acknowledgments

We thank Dakang Sun for Flow cytometry analysis and Hongliang Dong for transmission electron microscope assistance. We also thank Na Ni for valuable confocal microscopy assistance. Finally, we thank BioNovoGene for Quantitative proteomic analysis and bioinformatic analysis.

References

[1] S. Park, "Mechanical Alteration Associated With Chemotherapeutic Resistance of Breast Cancer Cells," *J Cancer Prev*, vol. 23, no. 2, pp. 87-92, 2018.

[2] W. Wang, Zou L., Zhou D., Zhou Z., Tang F., Xu Z.andLiu X., "Overexpression of ubiquitin carboxyl terminal hydrolase-L1 enhances multidrug resistance and invasion/metastasis in breast cancer by activating the MAPK/Erk signaling pathway," *Mol Carcinog*, vol. 55, no. 9, pp. 1329-1342, 2016.

[3] W. Jiang, Liu L.andChen Y., "Simultaneous Detection of Human C-Terminal p53 Isoforms by Single Template Molecularly Imprinted Polymers (MIPs) Coupled with Liquid Chromatography-Tandem Mass Spectrometry (LC-MS/MS)-Based Targeted Proteomics," *Anal Chem*, vol. 90, no. 5, pp. 3058-3066, 2018.

[4] H. Li, Meng F., Jiang L., Ren Y., Qiu Z., Yu P.andPeng J., "Comparison of LC-MS/MS-based targeted proteomics and conventional analytical methods for monitoring breast cancer resistance protein expression," *Life Sci*, vol. 231, pp. 116548, 2019.

[5] F. Meng, Zou L., Zhang T., Jiang L., Ding Y., Yu P.andPeng J., "Using LC-MS/MS-based targeted proteomics to monitor the pattern of ABC transporters expression in the development of drug resistance," *Cancer Manag Res*, vol. 10, pp. 2859-2870, 2018.

[6] M. Wu, Ye H., Shao C., Zheng X., Li Q., Wang L., Zhao M., Lu G., Chen B., Zhang J., Wang Y., Wang G.andHao H., "Metabolomics-Proteomics Combined Approach Identifies Differential Metabolism-Associated Molecular Events between Senescence and Apoptosis," *J Proteome Res*, vol. 16, no. 6, pp. 2250-2261, 2017.

[7] E. Bigagli, Cinci L., D'Ambrosio M.andLuceri C., "Transcriptomic Characterization, Chemosensitivity and Regulatory Effects of Exosomes in Spontaneous EMT/MET Transitions of Breast Cancer Cells," *Cancer Genomics Proteomics*, vol. 16, no. 3, pp. 163-173, 2019.

[8] T. B. Steinbichler, Dudas J., Skvortsov S., Ganswindt U., Riechelmann H.andSkvortsova I. I., "Therapy resistance mediated by exosomes," *Mol Cancer*, vol. 18, no. 1, pp. 58, 2019.

[9] A. Sharma, "Chemoresistance in cancer cells: exosomes as potential regulators of therapeutic tumor heterogeneity," *Nanomedicine (Lond)*, vol. 12, no. 17, pp. 2137-2148, 2017.

[10] O. Schillaci, Fontana S., Monteleone F., Taverna S., Di Bella M. A., Di Vizio D.andAlessandro R., "Exosomes from metastatic cancer cells transfer amoeboid phenotype to non-metastatic cells and

increase endothelial permeability: their emerging role in tumor heterogeneity," *Sci Rep*, vol. 7, no. 1, pp. 4711, 2017.

[11] X. Wang, Xu C., Hua Y., Sun L., Cheng K., Jia Z., Han Y., Dong J., Cui Y.andYang Z., "Exosomes play an important role in the process of psoralen reverse multidrug resistance of breast cancer," *J Exp Clin Cancer Res*, vol. 35, no. 1, pp. 186, 2016.

[12] J. C. Santos, Ribeiro M. L., Sarian L. O., Ortega M. M.andDerchain S. F., "Exosomes-mediate microRNAs transfer in breast cancer chemoresistance regulation," *Am J Cancer Res*, vol. 6, no. 10, pp. 2129-2139, 2016.

[13] C. Yang, Guo W. B., Zhang W. S., Bian J., Yang J. K., Zhou Q. Z., Chen M. K., Peng W., Qi T., Wang C. Y.andLiu C. D., "Comprehensive proteomics analysis of exosomes derived from human seminal plasma," *Andrology*, vol. 5, no. 5, pp. 1007-1015, 2017.

[14] X. Wang, Han Y., Liu J., Zhang Y., Cheng K., Guo J., Guo Q., Liu S., Sun H., Hua Y., Zhang G., Xu S., Guo F.andYang Z., "Exosomes Play an Important Role in the Progression of Plasma Cell Mastitis via the PI3K-Akt-mTOR Signaling Pathway," *Mediators Inflamm*, vol. 2019, pp. 4312016, 2019.

[15] S. Libregts, Arkesteijn G., Nemeth A., Nolte-'T H. E.andWauben M., "Flow cytometric analysis of extracellular vesicle subsets in plasma: impact of swarm by particles of non-interest," *J Thromb Haemost*, vol. 16, no. 7, pp. 1423-1436, 2018.

[16] Z. L. Yang, Cheng K.andHan Z. D., "Effect of bFGF on the MCF-7 Cell Cycle with CD44(+)/CD24(-): Promoting the G0/G1–>G2/S Transition," *J Breast Cancer*, vol. 15, no. 4, pp. 388-392, 2012.

[17] L. Mashouri, Yousefi H., Aref A. R., Ahadi A. M., Molaei F.andAlahari S. K., "Exosomes: composition, biogenesis, and mechanisms in cancer metastasis and drug resistance," *Mol Cancer*, vol. 18, no. 1, pp. 75, 2019.

[18] H. D. Zhang, Jiang L. H., Hou J. C., Zhong S. L., Zhu L. P., Wang D. D., Zhou S. Y., Yang S. J., Wang J. Y., Zhang Q., Xu H. Z., Zhao J. H., Ji Z. L.andTang J. H., "Exosome: a novel mediator in drug resistance of cancer cells," *Epigenomics*, vol. 10, no. 11, pp. 1499-1509, 2018.

[19] B. Kulkarni, Kirave P., Gondaliya P., Jash K., Jain A., Tekade R. K.andKalia K., "Exosomal miRNA in chemoresistance, immune evasion, metastasis and progression of cancer," *Drug Discov Today*, vol. 24, no. 10, pp. 2058-2067, 2019.

[20] M. Wang, Zhou L., Yu F., Zhang Y., Li P.andWang K., "The functional roles of exosomal long non-coding RNAs in cancer," *Cell Mol Life Sci*, vol. 76, no. 11, pp. 2059-2076, 2019.

[21] J. C. Santos, Ribeiro M. L., Sarian L. O., Ortega M. M.andDerchain S. F., "Exosomes-mediate microRNAs transfer in breast cancer chemoresistance regulation," *Am J Cancer Res*, vol. 6, no. 10, pp. 2129-2139, 2016.

[22] L. Bourguignon, "Matrix Hyaluronan-CD44 Interaction Activates MicroRNA and LncRNA Signaling Associated With Chemoresistance, Invasion, and Tumor Progression," *Front Oncol*, vol. 9, pp. 492, 2019.

[23] L. Bourguignon, Earle C.andShiina M., "Activation of Matrix Hyaluronan-Mediated CD44 Signaling, Epigenetic Regulation and Chemoresistance in Head and Neck Cancer Stem Cells," *Int J Mol Sci*, vol. 18, no. 9, 2017.

[24] L. Y. Bourguignon, Shiina M.andLi J. J., "Hyaluronan-CD44 interaction promotes oncogenic signaling, microRNA functions, chemoresistance, and radiation resistance in cancer stem cells leading to tumor progression," *Adv Cancer Res*, vol. 123, pp. 255-275, 2014.

[25] B. P. TooleandSlomiany M. G., "Hyaluronan, CD44 and Emmprin: partners in cancer cell chemoresistance," *Drug Resist Updat*, vol. 11, no. 3, pp. 110-121, 2008.

[26] Y. H. Quan, Lim J. Y., Choi B. H., Choi Y., Choi Y. H., Park J. H.andKim H. K., "Self-targeted knockdown of CD44 improves cisplatin sensitivity of chemoresistant non-small cell lung cancer cells," *Cancer Chemother Pharmacol*, vol. 83, no. 3, pp. 399-410, 2019.

[27] S. M. Kim, Yang Y., Oh S. J., Hong Y., Seo M.andJang M., "Cancer-derived exosomes as a delivery platform of CRISPR/Cas9 confer cancer cell tropism-dependent targeting," *J Control Release*, vol. 266, pp. 8-16, 2017.

Tables

Table 1 Down-regulated proteins in ADR/Exo (log2FoldChange|≧1.0)

ID	geneName	log2FC	p.value	FDR
Q8N139	ABCA6	-2.749913623	1.01E-20	1.27E-18
Q6UXH8	CCBE1	-2.568773782	7.06E-15	4.20E-14
Q15113	PCOLCE	-2.030636749	4.16E-20	3.02E-18
P42226	STAT6	-2.029372498	1.31E-17	1.75E-16
P28300	LOX	-1.964732595	2.11E-17	2.59E-16
Q92616	GCN1	-1.90252404	1.52E-12	5.61E-12
Q96JB1	DNAH8	-1.74259009	2.20E-16	1.99E-15
P45877	PPIC	-1.733721336	9.79E-17	9.92E-16
Q96JB3	HIC2	-1.641697244	4.05E-17	4.46E-16
Q9P2B2	PTGFRN	-1.641418313	8.64E-19	2.11E-17
P04196	HRG	-1.614183536	6.78E-19	1.81E-17
P09104	ENO2	-1.608579238	3.88E-17	4.32E-16
P02452	COL1A1	-1.540018335	2.26E-19	8.64E-18
Q9H444	CHMP4B	-1.458281503	3.59E-17	4.10E-16
P69891	HBG1	-1.410841247	2.43E-19	8.91E-18
Q92743	HTRA1	-1.407445068	2.32E-17	2.80E-16
P35527	KRT9	-1.286180149	1.39E-16	1.32E-15
P35442	THBS2	-1.281549857	4.80E-20	3.02E-18
Q8WUM4	PDCD6IP	-1.272078017	3.80E-21	6.70E-19
P04264	KRT1	-1.255475836	1.00E-17	1.47E-16
Q86UQ4	ABCA13	-1.235719556	4.95E-16	3.96E-15
P98095	FBLN2	-1.234047063	2.53E-18	5.02E-17
O00560	SDCBP	-1.228518401	1.16E-17	1.65E-16
O75787	ATP6AP2	-1.217030018	4.58E-16	3.74E-15
Q14644	RASA3	-1.197061891	3.46E-17	4.02E-16
P05543	SERPINA7	-1.194182102	3.87E-15	2.54E-14
P27169	PON1	-1.183708286	1.42E-15	1.03E-14
Q96IY4	CPB2	-1.18209426	5.65E-15	3.52E-14
Q8IUX7	AEBP1	-1.177460612	5.67E-15	3.52E-14
Q13163	MAP2K5	-1.166608274	7.20E-22	2.11E-19
Q9NQ79	CRTAC1	-1.153827418	4.49E-12	1.47E-11
Q9UBX5	FBLN5	-1.150018759	2.87E-18	5.33E-17
P22352	GPX3	-1.14279763	1.14E-15	8.60E-15
P08123	COL1A2	-1.12703972	5.74E-18	9.21E-17
P00734	F2	-1.123334375	6.85E-20	3.55E-18
P35908	KRT2	-1.118460938	1.14E-17	1.65E-16
P13645	KRT10	-1.103906127	2.02E-15	1.39E-14
P12110	COL6A2	-1.099515524	1.10E-14	6.23E-14
Q08830	FGL1	-1.089668388	2.36E-17	2.81E-16
Q03181	PPARD	-1.085861659	3.87E-16	3.22E-15
P51888	PRELP	-1.081786073	4.83E-12	1.57E-11

Q9UKL3	CASP8AP2	-1.062406911	2.12E-14	1.14E-13

Table 2 Up-regulated proteins in ADR/Exo (log2FoldChange|≧1.0)

ID	geneName	log2FC	p.value	FDR
P21589	NT5E	1.009819327	4.74E-14	2.35E-13
P63313	TMSB10	1.010447833	1.98E-13	8.62E-13
A0A0C4DH25	IGKV3D-20	1.01148149	8.14E-16	6.29E-15
P30530	AXL	1.019494342	1.02E-10	2.69E-10
P36873	PPP1CC	1.020861041	2.07E-06	3.15E-06
Q6Y7W6	GIGYF2	1.054584991	0.008236081	0.009792156
Q01469	FABP5	1.082601951	1.33E-12	4.99E-12
P07355	ANXA2	1.085642302	5.75E-18	9.21E-17
P05783	KRT18	1.089381553	3.56E-19	1.16E-17
P15311	EZR	1.092422023	1.16E-16	1.16E-15
P08183	ABCB1	1.100920565	1.80E-13	7.88E-13
P03956	MMP1	1.107720918	3.41E-16	2.89E-15
P29279	CTGF	1.111400029	3.13E-19	1.10E-17
P11234	RALB	1.132346931	4.82E-10	1.15E-09
P05362	ICAM1	1.136468428	5.81E-20	3.41E-18
O43707	ACTN4	1.137934567	1.69E-13	7.44E-13
Q9NZI8	IGF2BP1	1.137949597	1.06E-14	6.11E-14
P62318	SNRPD3	1.154095566	1.78E-17	2.28E-16
Q9BXJ9	NAA15	1.160094638	3.20E-10	7.89E-10
Q02952	AKAP12	1.165918327	3.42E-14	1.73E-13
Q14166	TTLL12	1.211203879	5.86E-17	6.22E-16
P13987	CD59	1.222304607	3.22E-23	1.42E-20
Q9HC35	EML4	1.232950225	5.39E-17	5.79E-16
P09936	UCHL1	1.254060267	1.28E-17	1.75E-16
P0DP24	CALM2	1.256303687	5.77E-15	3.53E-14
Q05639	EEF1A2	1.257059569	1.04E-09	2.32E-09
Q96KK5	HIST1H2AH	1.259356299	2.97E-14	1.54E-13
P31947	SFN	1.284978449	1.24E-16	1.22E-15
P01705	IGLV2-23	1.292466271	2.15E-21	4.75E-19
P04792	HSPB1	1.329895601	2.52E-18	5.02E-17
Q15485	FCN2	1.334237769	4.60E-19	1.45E-17
P80723	BASP1	1.34673813	2.91E-13	1.23E-12
P00739	HPR	1.376022578	2.91E-18	5.33E-17
P17813	ENG	1.406909301	6.51E-20	3.55E-18
P16070	CD44	1.507068654	7.13E-18	1.09E-16
P48509	CD151	1.511050753	9.36E-18	1.40E-16
Q9GZP8	IMUP	1.512574238	8.84E-21	1.27E-18
O95816	BAG2	1.554351074	2.29E-18	4.81E-17
P49006	MARCKSL1	1.574548865	2.00E-16	1.85E-15
Q16186	ADRM1	1.70465692	3.88E-09	8.03E-09
P31431	SDC4	1.852031808	1.52E-18	3.51E-17

P21926	CD9	1.948493353	7.11E-17	7.37E-16
P35613	BSG	2.103885514	5.82E-16	4.62E-15
P02795	MT2A	2.654815629	1.01E-13	4.68E-13

Figures

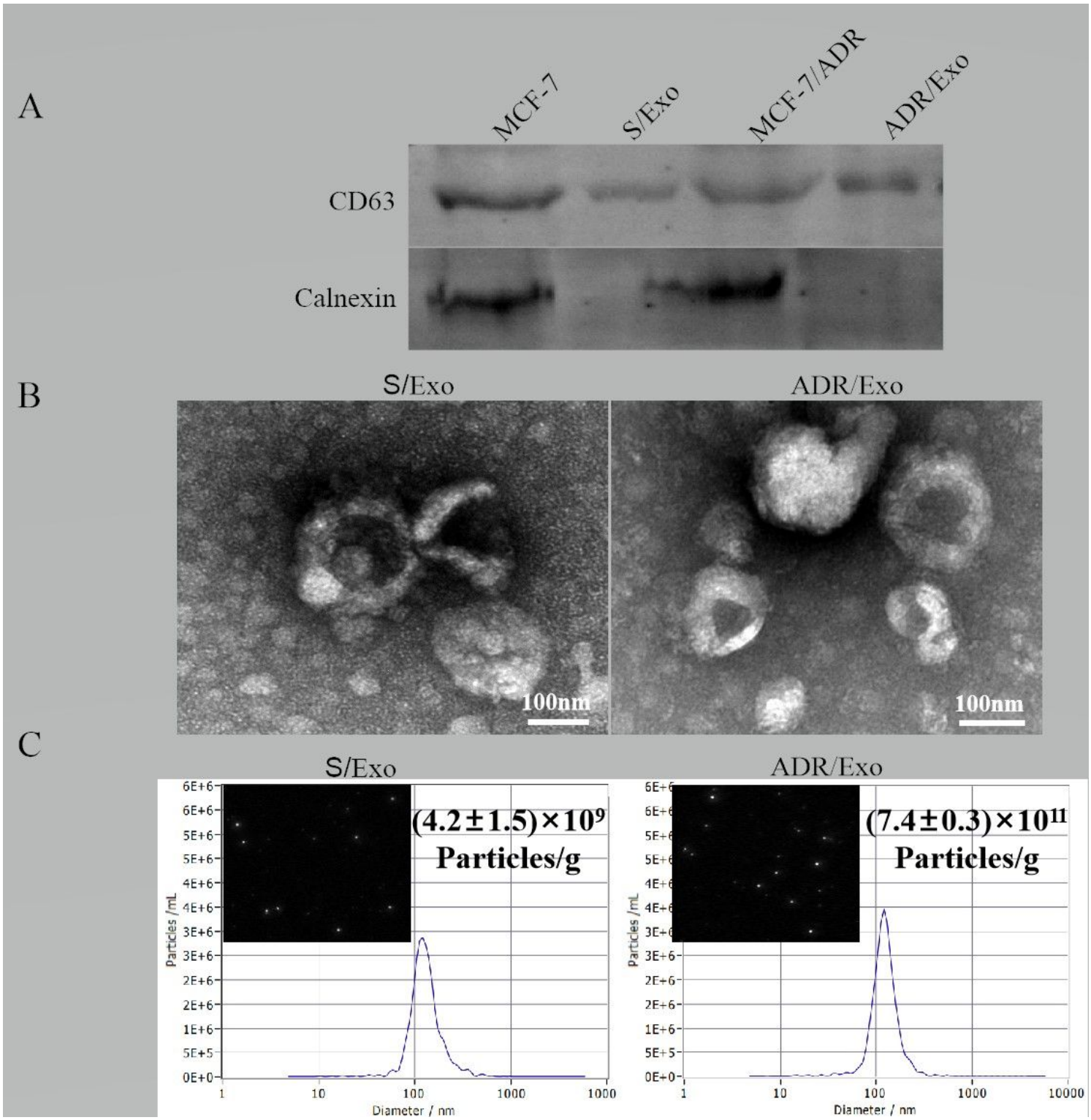

Figure 1

DOX increased the exosomes release of MCF-7/ADR cells. (A)These vesicles expressed conventional exosomal markers CD63, while calnexin was only detected in total cellular lysates and not in exosomes. (B) The morphology of exosomes was analyzed using TEM and (C) The size distribution and concentration of A/Exo and S/Exo were analyzed by NTA. There were no significant differences in morphology and size distribution between S/Exo and ADR/Exo ($p>0.05$) while the concentration of A/Exo was significantly higher than S/Exo ($p<0.05$).

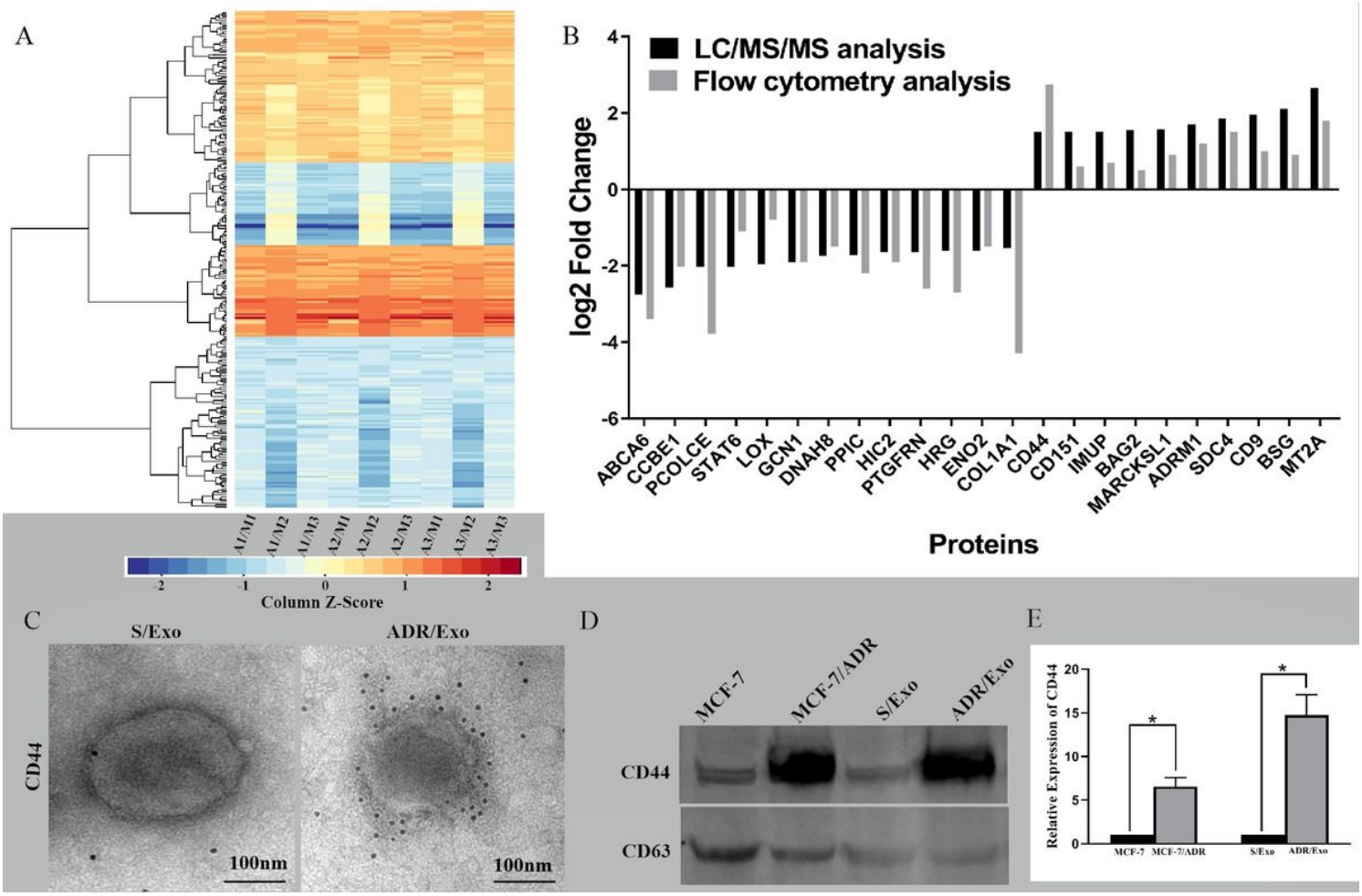

Figure 2

DOX-resistant breast cancer cells spread resistance capacity to sensitive ones by releasing exosomes to transfer resistance-associated proteins, especially CD44. (A) Heatmap of proteins that are differentially abundant in ADR/exo by proteomic analysis. (B) We further verified these differently expressed proteins by flow cytometry analysis which was consistent with the proteomic analysis and the CD44 has the most significant fold change. (C) Immunoelectron microscopy (IEM) showed that CD44 were highly stored inside ADR/exo. (D) and (E) Western blot results indicated that the protein level of CD44 was significantly up-regulated in ADR/exo compared with that in S/exo ($p<0.05$).

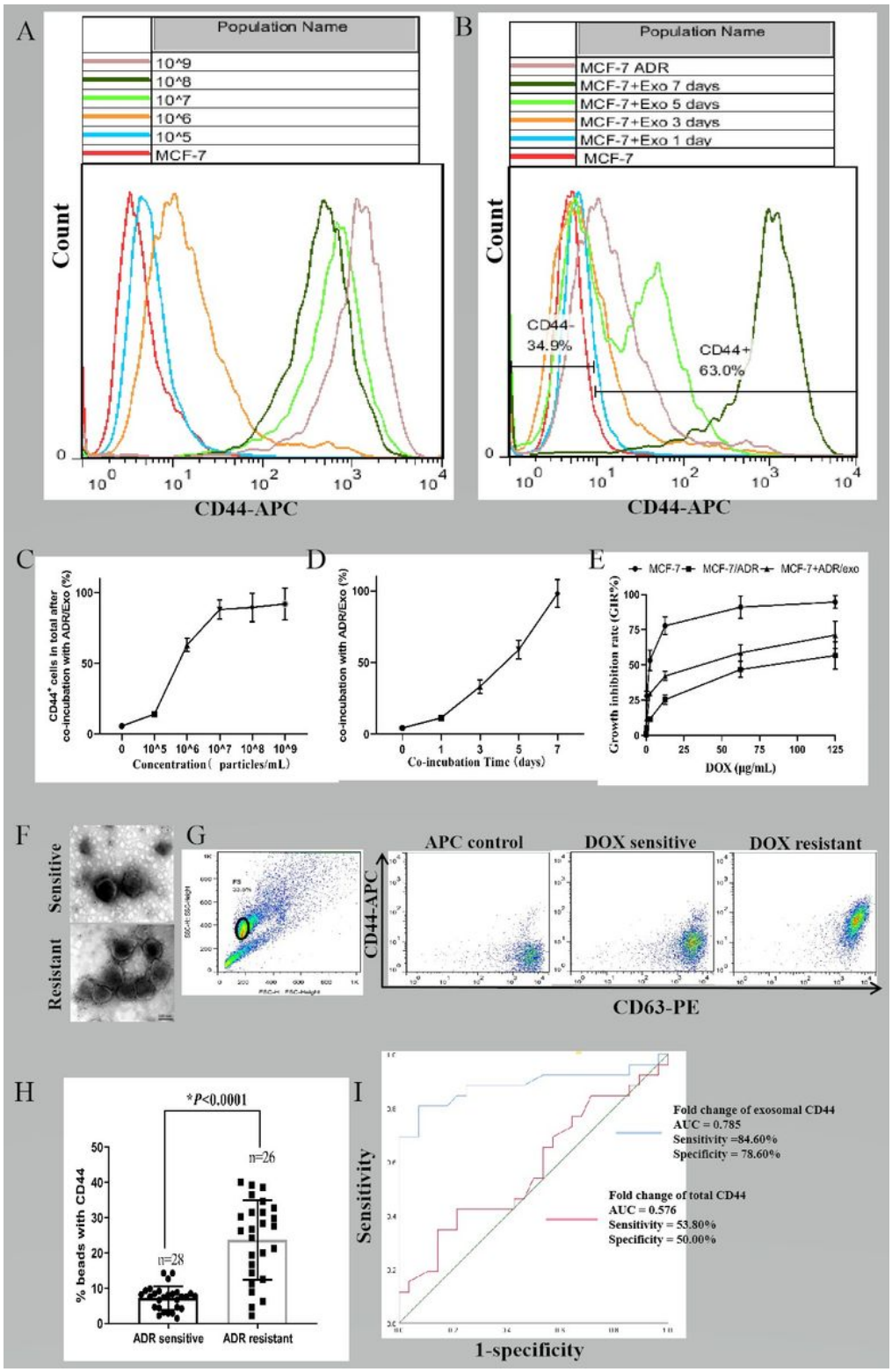

Figure 3

CD44 was transmited from MCF-7/ADR to MCF-7 cells via exosomes. ADR/Exo incubation increased the percentage of CD44 in MCF-7 cells in a concentration dependent manner (A) and time dependent manner (B). (C) The expression of CD44 in MCF-7+ADR/Exo with 1×105, 1×106, 1×107, 1×108 and 1×109 particles/mL was 5.73%±0.10%, 14.10%±0.70%, 63.00%±5.60%, 88.12%±9.70% and 92.0%±11.20% respectively. There was no significant differences between the 1×108 and 1×109 group (p>0.05) . (D) The

expression of CD44 in MCF-7+ADR/Exo at 0,1st, 3rd, 5th and 7th was 4.35%±0.71%, 11.42%±1.60%, 33.21%±4.70%, 58.90%±6.54% and 91.10%±9.66% respectively. (E) The DOX sensitivity of MCF-7 was significantly decreased after 7 days incubation with 1×108 particles/mL ADR/Exo. (F) Immunogold TEM results showed that exosomal CD44 in the serum of PD/SD was significantly higher than that in PR/CR. (G) Exosomes derived from PD/SD and PR/CR donor peripheral blood were pulled down on beads, stained with anti-CD63-PE and anti-CD44-APC, analyzed by flow cytometry. (H) Quantitative analysis of flow cytometry results. (I) ROC curves indicated that exosomal CD44 shows AUC=0.785, a sensitivity of 84.60% and a specificity of 78.60%, while serum CD44 shows an AUC of 0.576, a sensitivity of 53.80% and a specificity of 50.00% .

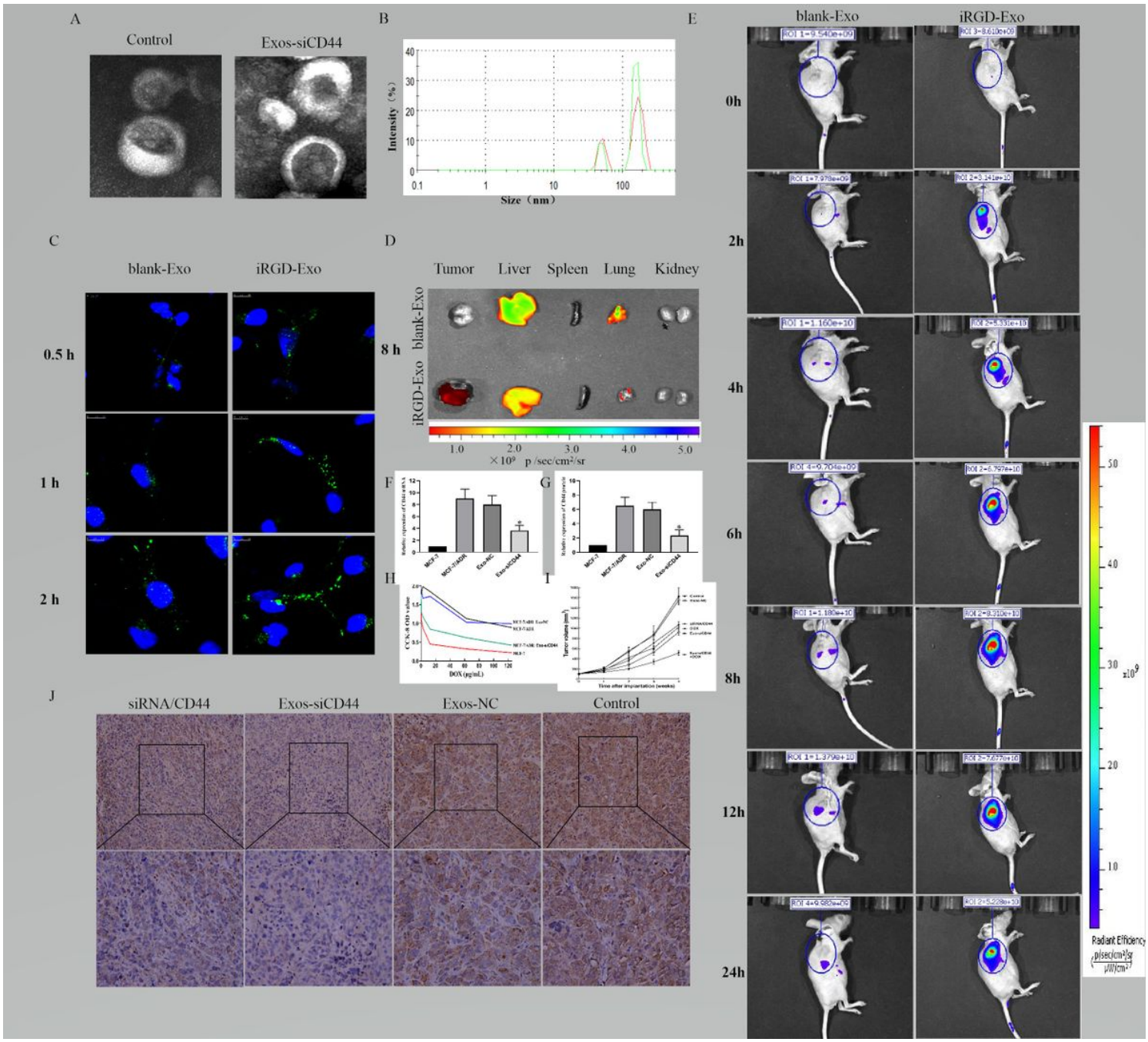

Figure 4

Modified exosome-mediated in vitro cellular uptake and in vivo bio-distribution. (A) TEM images showed that there were no significant changes in the morphological integrity after electroporation compared with the untreated exosomes. (B) NTA also showed that there were no significant difference in size compared with the untreated exosomes ($p>0.05$). (C) Confocal images exhibited that the uptake efficiency was higher in the presence of iRGD-Exo than that in the presence of blank-Exo by MFI ($p<0.05$). (D) Fluorescence intensity of DiD-labelled exosome at tumors and other tissues. The results showed that the iRGD-Lamp2b modification facilitated Exo targeting, the Exo being preferentially taken up by tumor cells, but also liver and, less efficiently, lung cells. (E) The vivo bio-distribution imaging showed that iRGD-Exo could efficiently and quickly target tumor cells. (F) The transferred CD44 siRNA by iRGD-Exo suffices for a significant reduction of CD44 expression in MCF-7/ADR cells. mRNA expression of CD44 in iRGD-Exos-siRNA/CD44 group was significantly reduced compared with the Exos-NC group and untreated MCF-7/ADR group ($p<0.05$). (G) Western blot results also showed that CD44 was reduced markedly in iRGD-Exos-siRNA/CD44 group ($p<0.05$). (H) CCK-8 cell proliferation assay revealed that iRGD-Exos-siRNA/CD44 increased chemo-sensitivity of DOX in MCF-7/ADR cells. (I) Tumor volumes data indicated the anti-tumor efficacy of iRGD-Exos-siRNA/CD44. (J) Immunohistochemistry results showed that the expression of CD44 was significantly decreased in iRGD-Exos-siRNA/CD44 group compared with other groups.

Supplementary Files

This is a list of supplementary files associated with this preprint. Click to download.

- Supplementdate2KEGGenrichment.png
- Supplementdate1GOenrichment.png